Title	Isotopic variation of molecular hydrogen in 20° –375°C hydrothermal fluids as detected by a new analytical method
Author(s)	Kawagucci, Shinsuke; Toki, Tomohiro; Ishibashi, Junichiro; Takai, Ken; Ito, Michihiro; Oomori, Tamotsu; Gamo, Toshitaka
Citation	Journal of Geophysical Research: Biogeosciences, 115(G3)
Issue Date	2010-08-28
URL	http://hdl.handle.net/20.500.12000/37628
Rights	©2010. American Geophysical Union.

Isotopic variation of molecular hydrogen in 20°–375°C hydrothermal fluids as detected by a new analytical method

Shinsuke Kawagucci,[1,2] Tomohiro Toki,[3] Junichiro Ishibashi,[4] Ken Takai,[2,5] Michihiro Ito,[3] Tamotsu Oomori,[3] and Toshitaka Gamo[1,6]

[1] Molecular hydrogen (H_2) is one of the most important energy sources for subseafloor chemolithoautotrophic microbial ecosystems in the deep-sea hydrothermal environments. This study investigated stable isotope ratios of H_2 in 20°–375°C hydrothermal fluids to evaluate usefulness of the isotope ratio as a tracer to explore the H_2-metabolisms. Prior to the observation, we developed an improved analytical method for the determination of concentration and stable isotope ratio of H_2. This method achieved a relatively high sensitivity with a detection limit of 1 nmol H_2 within an analytical error of 10‰ in the δD_{H2} value. The δD_{H2} values in the high-temperature fluids were between −405‰ and −330‰, indicating the achievement of the hydrogen isotopic equilibrium between H_2 and H_2O at around the hydrothermal end-member temperature. In contrast, several low-temperature fluids showed apparently smaller δD_{H2} values than those in the high-temperature fluids in spite of a negligible δD_{H2} change due to fluid-seawater mixing, suggesting the possibility of δD_{H2} change in the low-temperature fluids and the surrounding environments. Since the δD_{H2} change in low-temperature environments is not well explained by the very sluggish abiotic thermal isotopic equilibrium between H_2 and H_2O, it could be associated with (micro)biological H_2-consuming and/or H_2-generating metabolisms that would strongly promote the isotopic equilibrium at low temperatures. Our first detection of the δD_{H2} variation in deep-sea hydrothermal systems presents the availability of the δD_{H2} value as a new tracer for microbes whose enzymes catalyze D/H exchange in H_2.

1. Introduction

[2] Subseafloor low temperature hydrothermal environments are formed by mixing between hot, reducing hydrothermal fluids and cool, oxidizing seawater prior to emissions from the seafloor. Because the environments have steep physical and chemical gradients and provide a variety of redox couples for chemolithotrophic microbial activities [e.g., *McCollom and Shock*, 1997], low-temperature hydrothermal fluids (LTHFs), defined as fluids venting from seafloor after the subseafloor mixing, are more or less altered by the microbial functions at the subseafloor environments [e.g., *Butterfield et al.*, 2004; *Toki et al.*, 2008]. Thus, the com-

parative investigations of the compositional and isotopic chemistry between LTHFs and high-temperature hydrothermal fluids (HTHFs), close to the end-member fluids, have provided important clues to the potential chemolithoautotrophic activities in the subseafloor hydrothermally mixing zones [*von Damm and Lilley*, 2004].

[3] Molecular hydrogen, H_2, is enriched in hydrothermal fluids, especially at ultramafic-hosted hydrothermal systems, and hydrothermal H_2 is considered to be a natural clean energy source [e.g., *Charlou et al.*, 2002]. Moreover, several theoretical investigations and geochemical and microbiological characterizations of practical fields strongly suggested that H_2 is one of the most important energy sources for subseafloor chemolithoautotrophic microbial ecosystems in the deep-sea hydrothermal environments because of its metabolic diversity even to reduce CO_2 [*McCollom and Shock*, 1997; *Takai et al.*, 2004]. In particular, hydrogenotrophic methanogenesis is thought as a key metabolism for sustaining active subseafloor ecosystems in the modern Earth and even ancient or extraterrestrial ecosystems [*McCollom*, 1999; *Takai et al.*, 2006; *Ueno et al.*, 2006]. Although the detection of isotopic anomaly of methane in various temperatures of hydrothermal fluids [*Takai et al.*, 2004; *Proskurowski et al.*, 2008] has been proposed as signatures for hydro-

[1]Ocean Research Institute, University of Tokyo, Tokyo, Japan.
[2]Precambrian Ecosystem Laboratory, Japan Agency for Marine-Earth Science and Technology, Yokosuka, Japan.
[3]Faculty of Science, University of the Ryukyus, Nishihara, Japan.
[4]Faculty of Sciences, Kyusyu University, Higashi, Japan.
[5]Subsurface Geobiology Advanced Research Project, Japan Agency for Marine-Earth Science and Technology, Yokosuka, Japan.
[6]Now at Atmosphere and Ocean Research Institute, University of Tokyo, Kashiwa, Japan.

genotrophic methanogenesis providing the ^{13}C-depleted methane, the ^{13}C-depleted abiotic methane [*McCollom and Seewald*, 2006] and ^{13}C-enriched biogenic methane [*Takai et al.*, 2008b] have been recently reported. In addition, the stoichiometric and isotopic composition of methane [e.g., *Proskurowski et al.*, 2008] could provide only implication for microbial methanogenesis among diverse H$_2$-dependent chemolithotrophic metabolisms. Thus in order to explore the diverse microbial H$_2$-metabolisms such as hydrogenotrophic chemolithoautotrophs and fermentative hydrogenogenesis in the deep-sea hydrothermal environments, another possible tracer is very useful.

[4] A stable hydrogen isotope ratio of H$_2$ (δD$_{H2}$) may be a candidate of the tracer for the H$_2$-consuming and -generating metabolisms of the microbial communities. The recently developed methods using continuous flow isotope ratio mass spectrometry (CF-IRMS) have provided the sensitive and accurate determination of δD$_{H2}$ values in the natural gas samples [*Rahn et al.*, 2002; *Rhee et al.*, 2004]. Nevertheless, the δD$_{H2}$ data in the hydrothermal environments are still very limited to the ones from the HTHFs in several hydrothermal systems (EPR21°N [*Welhan and Craig*, 1983]; EPR13°N [*Merlivat et al.*, 1987]; EPR9°N, Logatchev, Broken Spur, Kairei, Guaymas, Endeavor, and Middle Valley [*Proskurowski et al.*, 2006]), except for the Lost City hydrothermal field at which venting fluids contain H$_2$ more than 1 mmol/kg even at low temperature [*Proskurowski et al.*, 2006]. The limited data set is evidently caused by the methodological limitation that could determine the relatively high concentrations of H$_2$ in the hydrothermal fluid samples. The methods using CF-IRMS could have much higher sensitivities [e.g., *Kawagucci et al.*, 2005] and would be applicable to the LTHFs containing considerably lower concentrations of H$_2$ than the HTHFs.

[5] The δD$_{H2}$ in geothermal and hydrothermal fluid systems has been widely used as a geochemical thermometer [e.g., *Arnason*, 1977; *Proskurowski et al.*, 2006] but rarely as a tracer for (micro)biological activity. The availability of δD$_{H2}$ as a thermometer is based on a hydrogen isotopic equilibrium (exchange) between H$_2$ and H$_2$O, which shows a temperature dependency represented by the following equation [*Horibe and Craig*, 1995].

$$HHO + HD \leftrightarrow HDO + HH$$
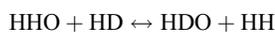
$$\alpha_{[H2O\text{-}H2]} = 1.0473 + 201036/T^2 + 2.060 \times 10^9/T^4 \\ + 0.180 \times 10^{15}/T^6 \qquad (1)$$

In this equation, $\alpha_{[H2O\text{-}H2]}$ represents $(D/H)_{H2O}/(D/H)_{H2}$ and T represents temperature (Kelvin). The isotopic equilibrium is usually achieved in natural sub(sea)floor thermal fluids because of long residence time while the isotope exchange is negligible over a month at the ambient temperature without any catalyst [*Campbell et al.*, 2009]. Moreover, enzymes involving microbial H$_2$ consumption are known to serve as a catalyst activating the isotope exchange between H$_2$ and H$_2$O [e.g., *Vignais*, 2005], and to bring about the isotopic equilibrium even at ambient temperature [*Romanek et al.*, 2003; *Valentine et al.*, 2004; *Campbell et al.*, 2009], although most of the microbial processes also induce a kinetic isotope fractionation. The isotopic equilibrium at temperatures lower than 120°C was represented by the δD$_{H2}$ values obtained from

the Lost City hydrothermal fluids, which was possibly affected by hydrogenotrophic microbial metabolism [*Proskurowski et al.*, 2006].

[6] In this study, we successfully developed a simple and highly sensitive analytical method for determination of H$_2$ concentration and δD$_{H2}$ value. This method enables us to measure δD$_{H2}$ values in LTHFs that have low concentration of H$_2$. This study focuses on the difference of δD$_{H2}$ values between HTHFs and LTHFs in each hydrothermal field, if it exists, and understanding a reason of the difference for the purpose to evaluate an availability of δD$_{H2}$ value as a tracer for microbial H$_2$ metabolisms.

2. Site Description

[7] The following are brief explanations of the deep-sea hydrothermal fields investigated in this study. The hydrothermal fluids in the Kairei field in the Central Indian Ridge (CIR) [*Gamo et al.*, 2001; *Gallant and von Damm*, 2006] are characterized by H$_2$ concentration more than 1 mmol/kg most likely resulting from serpentinization of ultramafic rocks [*Kumagai et al.*, 2008; *Nakamura et al.*, 2009] and possible subseafloor microbial hydrogenotrophic methanogenesis [*Takai et al.*, 2004]. The end-member fluids in the Edmond field in the CIR [*van Dover et al.*, 2001] show H$_2$ concentrations similar to those in the fluids from other basalt-hosted MOR hydrothermal systems [*Kumagai et al.*, 2008]. The Hatoma Knoll hydrothermal field is located in a volcanic caldera in the Okinawa Trough (OT), a sediment-covered backarc basin. Bubbles and liquid CO$_2$ are vented with hydrothermal fluids due to subseafloor boiling of the fluid [*Nakano et al.*, 2001]. The Mariner hydrothermal field is located in the Valu Fa Ridge of the southern Lau Basin (LB) [*Takai et al.*, 2008a]. Vigorous black smokers and clear diffusing fluids have been observed. Possible H$_2$-, Sulfur-, and CH$_4$-oxidation of subseafloor microbial communities were suggested based on the geochemical and microbiological characterization [*Takai et al.*, 2008a].

3. Methods

3.1. Sampling Procedures

[8] All hydrothermal fluid samples were retrieved and treated in a similar manner as described below. Hydrothermal fluid samples were collected using a gas-tight fluid sampler *WHATS II* [*Saegusa et al.*, 2006] equipped to the ROV *Hyper Dolphin* during the cruise of R/V *Natsushima* (for the OT Hatoma Knoll field) or equipped to the submersible *Shinkai 6500* during the cruises of R/V *Yokosuka* (for the other fields). The gas-tight fluid sampler *WHATS II* brings the hydrothermal fluid samples on board while retaining the in situ gas composition, including H$_2$ [*Tsunogai et al.*, 2005; *Konno et al.*, 2006; *Saegusa et al.*, 2006]. The hydrothermal fluid temperature was monitored simultaneously at the fluid sampling using a temperature probe at the top of the fluid inlet tube. A fluid taken through a Teflon tubing [*Saegusa et al.*, 2006] was conductively cooled by deep-seawater surrounding the sampling system and kept at the low temperature in ~150 mL stainless-steel gas-tight bottles (WHATS bottle) until onboard processing. After recovery onboard, the fluids in the WHATS bottles were immediately opened to a vacuum line (ca. 1500 mL) to recover the gas
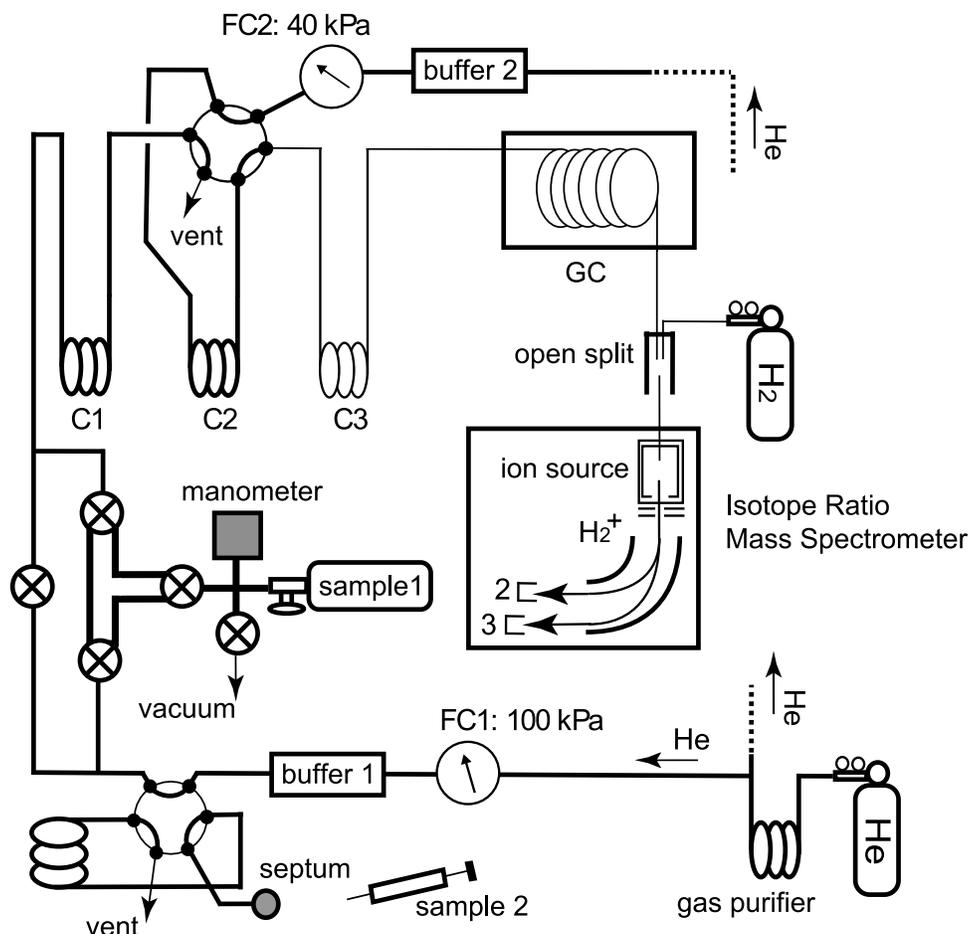
Figure 1. A schematic diagram of an analytical system for H_2 concentration and its δD, based on continuous flow isotope ratio mass spectrometry. Almost the entire flow path is produced using stainless steel tubes (bold line), although the flow path from C3 to the mass spectrometer is made using a capillary tube (thin line). The abbreviations are defined as follows: C1, a stainless steel tube packed column (Molecular Sieve 5A, 60/80 mesh, length = 2 m, I.D. = 2.17 mm); C2, a stainless steel tube packed column (Molecular Sieve 5A, 60/80 mesh, length = 50 cm, I.D. = 2.17 mm); C3, a capillary column (Molsieve 5A PLOT, length = 3 m, I.D. = 0.53 mm); GC, a GC capillary column (Molsieve 5A PLOT, length = 25 m, I.D. = 0.53 mm); FC1 and FC2, flow controllers.

components. Reagent-grade solid sulfamic acid ($HOSO_2NH_2$) and mercury chloride ($HgCl_2$) were added to the fluid in the vacuum line, respectively, to extract CO_2 and to remove H_2S as HgS. After degassing for 10 min., the gas phase were collected into 50 mL glass ampoules (in a case of the LB field) or 50 mL stainless bottles (in cases of the other fields) for H_2 and CO_2 analyses, at the same time all of the filtered (using a 0.45 μm pore size filter) liquid phase were also collected, for the subsequent onshore magnesium measurements by ICP-AES. Control experiments using degassed water and our water sampler bottles indicated the detection of less than 30 nmol/kg of H_2 with δD_{H2} values lower than -900‰ as the H_2 blank.

3.2. Development of a New Analytical Method for δD_{H2}

[9] The CF-IRMS system used in this study is based on *Rhee et al.* [2004]. A particular modification from the method by *Rhee et al.* [2004] was not to use the liquid helium device for H_2 purification: the newly developed method only

uses commercial columns and general refrigerants for H_2 purification on a carrier gas stream (Figure 1). This modification made the analytical procedure less laborious. In addition to the above modification, some minor differences between the previous and present methods may be found. The analytical procedure using the system is the following (Figure 1). First, an aliquot of the gas sample is introduced via a preevacuated line (sample 1), sometimes via a sample loop using a gas-tight syringe (sample 2), into the first carrier gas stream. The gas stream is of ultra-pure helium (purity is > 99.9999%: Japan Air Gases) further purified by a Molecular Sieve 5A column at LqN_2 temperature and preserved at a flow pressure of 100 kPa by a flow controller (FC1). To maintain a stable flow pressure, empty volumes for pressure buffers (buffer 1 and buffer 2) are built upstream of the sample path. The sample gas is cleaned up by eliminating H_2O, CO_2, and some N_2 and O_2 through a coolpacked column (C1) immersed in an ethanol-LqN_2 bath of around 173 K; then H_2 and the other residual gases are
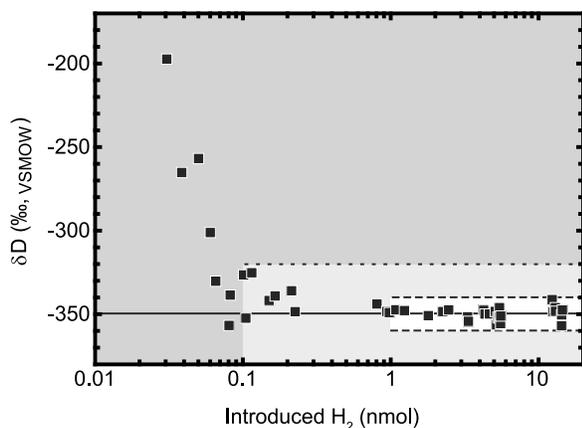
Figure 2. Determined δD_{H2} values plotted as a function of the amount of introduced H$_2$ using the method newly developed in this study. The x axis is presented in logarithm scales. A horizontal solid line represents the known δD_{H2} value of the H$_2$ used in the experiment (−349.5‰). White and light-gray zones represent highly precision (<±10‰ at >1 nmol introduction) and low precision analyses (<±30‰ at >0.1 nmol introduction), respectively.

trapped on a cold-packed column (C2) immersed in LqN$_2$. After the position of the six-port valve is rotated and the carrier stream is changed to a gas chromatograph at a flow pressure of 40 kPa (FC2), the sample gas trapped on the cold column (C2) is released at room temperature and soon reconcentrated on a capillary column trap (C3) at LqN$_2$ temperature. Finally, the sample gas on the capillary trap (C3) is released at room temperature and injected into the main gas-chromatograph capillary column (GC) for complete separation of H$_2$ from the other gas species. The effluent gas was introduced through an open split into an isotope ratio mass spectrometer (DELTA^{PLUS}XP; Thermo Finnigan) to determine the H$_2$ concentration and δD.

[10] To examine the analytical performance of our method, repeated analyses of the δD-known H$_2$ gas in a canister (−349.5‰) were carried out with barometrical dilution of H$_2$ by ultra-pure helium. The analytical precision for determining the H$_2$ concentration was estimated within 5%, which is comparable to the other CF-IRMS measurement (e.g., 2% [Rhee et al., 2004]). The relationship between the amount of introduced H$_2$ determined barometrically and the measured δD_{H2} value was investigated (Figure 2). The relationship indicated that the newly developed method could detect the δD_{H2} value within an analytical error of 10‰ at more than 1 nmol H$_2$ injection (Figure 2). As compared to the sensitivity attained by the previous method (detection limit of ca. 8 nmol H$_2$ within the error of 10‰ [Rhee et al., 2004]), the new technique was more sensitive. Although a blank was undetectable at empty gas bottle analyses by the procedure described above, larger deviations of δD_{H2} values at fewer H$_2$ introduction (Figure 2) suggests a small blank, less than 0.03 nmol-H$_2$, having a δD_{H2} value of around −200‰. The H$_2$ blank may come from carrier gases in spite of the careful purification. If a less precise analysis is permitted, only 0.1 nmol H$_2$ is enough to determine δD_{H2} value with an analytical error of 30‰ (Figure 2). The δD_{H2} value

of a sample gas was standardized using two commercial δD-known H$_2$ (−758.22‰ and −11.09‰; Shoko Co., Ltd.) for accurate determination.

4. Results

[11] The H$_2$ concentrations in the hydrothermal fluids from each field mostly demonstrated an inverse linear correlation with the Mg concentrations (Figure 3). Because of depletion of magnesium in end-member high-temperature hydrothermal fluid ([Mg] = 0 mmol/kg) while ~53 mmol-Mg/kg in seawater [von Damm, 1995], a linear correlation on the Mg diagram indicated a simple two end-member mixing between HTHF and seawater. The observed linear correlations thus demonstrated that the hydrothermal end-member fluid serve as the main H$_2$ source for the obtained fluids and that the H$_2$ concentration in each fluid sample was controlled primarily by dilution of the end-member fluid with H$_2$-depleted seawater. Molecular hydrogen concentrations in the LTHF samples ID933-1, ID934-2, and ID842-1 were considerably lower than those expected from the Mg-H$_2$ correlation (Table 1). The samples showing lower H$_2$ concentration anomalies also had lower H$_2$/CO$_2$ ratios (Table 1). The decrease of H$_2$/CO$_2$ ratio with the decrease of H$_2$ concentration suggests selective H$_2$ removal rather than whole dissolved gas stripping through the phase separation that little changes H$_2$/CO$_2$ ratio. Liquid CO$_2$ concomitant at fluid sampling can decrease H$_2$/CO$_2$ ratio due to CO$_2$ input, but increase H$_2$ concentration because of H$_2$ enrichment in the liquid CO$_2$ [Konno et al., 2006], whereas fermentative metabolisms at dense animal colony (Table 1) can generate both H$_2$ and CO$_2$ resulting in increases of H$_2$ concentration. Processes potentially controlling H$_2$ concentration in seawater environment, such as photochemical H$_2$ production [Punshon and Moore, 2008a] and H$_2$ generation associated
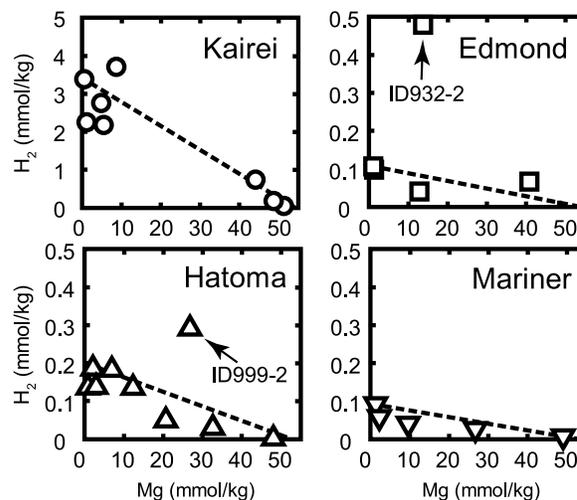

Figure 3. Magnesium-H$_2$ concentrations diagram of the various temperatures of hydrothermal fluids. Dashed lines are mixing lines between the highest-temperature fluid and the ambient seawater in each field. Arrows point to the samples that significantly deviated from the inverse correlation line between Mg and H$_2$ in the Edmond and the Hatoma fields.

Table 1. Summary of Samples Used and Data Measured in This Study[a]

Location	Field	Vent	ID	Max. T (°C)	Mg (mmol/kg)	H_2 (mmol/kg)	δD (‰)	CO_2 (mmol/kg)	H_2/CO_2 (*10^3)	Sample Description
CIR	Kairei	Kali	928–2	362	0.2	3.33	−368	8.0	415	H; black smoker fluid
		Monju	928–4	299	5.2	2.13	−385	7.9	268	H; black smoker fluid
		Fugen	929–2	305	4.5	2.71	−391	9.5	284	H; black smoker fluid
		Monju	933–1	42	50.9	0.0008	−431	9.3	0.1	L; clear diffusing flow fluid
		Monju	933–2	87	43.7	0.69	−361	6.0	114	L; fluid in the *Alviniconcha* gastropod colonies[b]
		Monju	934–2	22	48.3	0.13	−493	12.6	10	L; fluid in the scaly foot gastropod colonies
		Kali	934–3	316	8.4	3.65	−328	12.1	303	H; black smoker fluid
		Daikoku (Mrk#30)	936–2	306	0.8	2.20	−340	ND[c]		H; black smoker fluid
	Edmond	Nura1	930–2	375	0.6	0.11	−362	12.7	9	H; black smoker fluid
		White Head	931–2	263	12.4	0.04	−412	8.1	5	L; clear diffusing flow fluid
		Mrk#27	931–4	325	0.7	0.10	−377	12.1	8	H; black smoker fluid
		Grand Shrimp Valley	932–2	281	13.4	0.48	−681	12.1	40	L; fluid in the *Rimicaris* shrimp colonies[b]
		Mrk#24	932–4	116	40.6	0.07	−476	8.7	8	L; clear diffusing flow fluid
OT	Hatoma	Mrk#58	999–2	321	26.2	0.30	−391	322	0.9	H; clear smoker fluid
		Mrk#58	1000–1	319	2.2	0.15	−386	315	0.5	H; clear smoker fluid
		Mrk#58	1000–3	208	0.1	0.14	−373	394	0.4	H; bubbling flow fluid
		Mrk#59	1001–2	255	11.9	0.15	−388	64	2.3	H; clear smoker fluid
		C-2	D866–2	21	47.9	0.01	−373	26	0.4	L; fluid above the Paralvinella colonies
		C-2	D872–1	307	1.6	0.20	−369	661	0.3	H; clear smoker fluid
		C-2	D872–2	307	6.5	0.19	−366	437	0.4	H; clear smoker fluid
		Chura	D871–2	226	20.4	0.06	−401	95	0.6	H; clear smoker fluid
		Chura	D871–3	178	32.3	0.04	−403	65	0.6	H; clear smoker fluid
LB	Mariner	Snow	840–1	361	1.6	0.09	−340	36.1	2.4	H; black smoker fluid
		Crab restaurant	841–1	276	2.9	0.04	−374	69.6	0.6	H; black smoker fluid
		Unicorn	841–3	275	10.1	0.04	−368	ND		H; black smoker fluid
		Barnacle	848–1	179	27.3	0.02	−450	33.1	0.6	L; grayish smoker fluid
		Pagoda	842–1	25	49.6	0.0003	−632	ND		L; clear diffusing flow fluid

[a]CIR, Central Indian Ridge; OT, Okinawa Trough; LB, Lau Basin. "Max. T" refers to the maximum fluid temperature obtained during the fluid sampling. "H" and "L" under "sample description" represent HTHFs and LTHFs, respectively. The data of CO_2 concentrations in both the CIR fields and the LB field are from the previous studies by *Kumagai et al.* [2008] and *Takai et al.* [2008a, 2008b], respectively.
[b]Mixed with a nearby black smoker.
[c]ND, not determined.

with nitrogen fixation metabolism [*Punshon and Moore*, 2008b], should be negligible at nutrient-enriched dark deep-seawater. In contrast, the high H_2 consumption potential of microbial communities (e.g., consumption-rate constants of 0.14~8.67 day^{-1} [*Punshon et al.*, 2007]) can account for the decrease of both H_2 concentration and H_2/CO_2 ratio. Thus the negative H_2 concentration anomalies with negative H_2/CO_2 ratio anomalies would most likely be due to the microbial H_2 consumption in the mixed low-temperature fluids. Only the samples obtained from very dense animal colonies (*Rimicaris* shrimp) in the CIR Edmond field (ID932-2 in Table 1) and from clear smoker fluid at the OT Hatoma field (ID999-2 in Table 1) showed approximately 5 and 3 times higher H_2 concentrations than those expected from the Mg-H_2 correlation, respectively (Figure 3). Reasons for these positive anomalies are discussed below with stable isotope ratios.

[12] All the δD_{H2} values in the vigorously venting fluids, HTHFs (Table 1), were in the narrow range of −405‰ to −330‰ in spite of variable H_2 concentrations among the fields (Table 1). These values are consistent with the theoretical values (discussed below) and similar to those previously observed [*Proskurowski et al.*, 2006], supporting accurate δD_{H2} determination on our sampling and analytical procedures. In contrast, six samples (ID933-1, ID934-2,

ID932-2, ID932-4, ID842-1, and ID848-1) showed considerably small δD_{H2} values (<−405‰: Table 1). All six samples were LTHFs and would be influenced by processes in the subseafloor low-temperature environment formed by the dilution of HTHFs.

5. Discussion

5.1. Relationship Between Hydrothermal Fluid δD_{H2} and Temperature

[13] To examine the thermal isotopic equilibrium model between H_2 and H_2O in hydrothermal fluids [*Proskurowski et al.*, 2006], the relationship between the determined δD_{H2} values and the measured maximum temperature of fluids was analyzed (Figure 4). All the δD_{H2} values in the HTHFs were comparable or larger than −405‰ corresponding to a theoretically equilibrated δD_{H2} value based on equation (1) assuming $\delta D_{H2O} = +0‰$ [*Shanks et al.*, 1995] in the case when the fluid temperature is 300°C. This finding suggests that the δD_{H2} values in the HTHFs are controlled by the equilibrium at the temperature of hydrothermal end-member fluid and little changed after fluid cooling to below 300°C. The maximum δD_{H2} value of −328‰ is comparable with a theoretically equilibrated δD_{H2} value at the critical point temperature (407°C) assuming that the equation (1) is
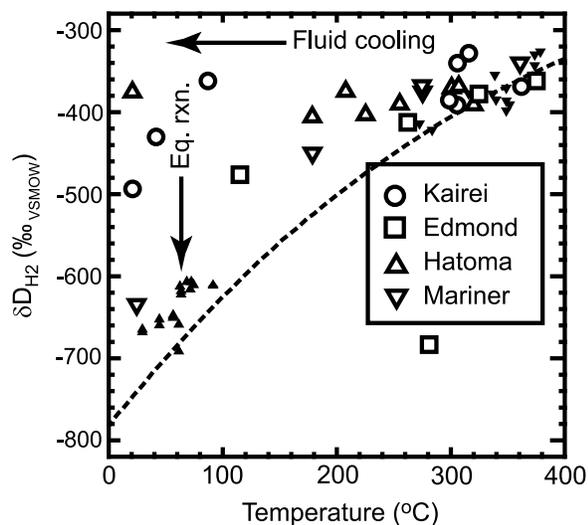
Figure 4. Relationship between the δD_{H2} values and the fluid temperature at the sampling. Open symbols indicate the data in this study. Solid triangles represent the previous data obtained from the high temperatures of hydrothermal fluids in the MOR hydrothermal systems (inversed) and the fluids from the Lost City hydrothermal field (normal) by *Proskurowski et al.* [2006]. Theoretically calculated δD_{H2} values assuming $\delta D_{H2O} = +0‰$ for equation (1) are also shown as a dashed curve. Fluid cooling and the subsequent isotope equilibrium reaction shift the plot to the left and down, respectively.

adaptable at the temperature. The observed range of δD_{H2O} values in hydrothermal systems (0 ± 5‰ [*Shanks et al.*, 1995]) little affects the calculation of equilibrated δD_{H2} values using equation (1) on the assumption and can be safely ignored for the purpose of this discussion. The low-temperature exposure of sampled fluids in the WHATS bottles until the onboard processing may induce the δD_{H2} change because the isotope exchange reaction was potentially catalyzed by a stainless steel inner wall of the WHATS bottle. If the hydrogen isotope exchange reaction occurred in the WHATS bottle after the sampling, the results plotted on the T-δD_{H2} plot (Figure 4) would be located below the theoretical curve due to the smaller equilibrated δD_{H2} value at lower temperature while the constant in situ (measured) temperature. Thus the results of the HTHF observation, plotted above or nearly on the curve (Figure 4), suggested negligible δD_{H2} change after the sampling.

[14] The samples of the LTHFs excluding ID932-2 (Table 1) are plotted on the left side far from the theoretical curve (Figure 4). The deviation from the curve means occurrence of isotope disequilibrium at the in situ (measured) temperature. The D-enriched δD_{H2} values, comparable with those in the HTHFs, at the lower in situ temperatures can be simply explained by a rapid temperature decrease resulting from dilution of HTHFs with cool ambient seawater (Figure 4). Since the H₂ concentrations in these fluids (~300 nmol/kg) are at least thousands of times higher than those in the ambient seawater (<0.1 nmol/kg [*Moore et al.,* 2009]), the conservative fluid-seawater mixing should have minimum affect on the

δD_{H2} values and can be safely ignored for the purpose of this discussion. In contrast, the samples showing the D-depleted H₂, compared to those in the HTHFs, at the lower in situ temperatures could not be explained by the conservative fluid-seawater mixing alone. It suggests that some processes at the subseafloor low-temperature environment changed isotopic composition of H₂ as well as the changes of carbon isotopic composition of methane at subseafloor low-temperature hydrothermal environments due to the microbial methanotrophs and methanogenesis [*Proskurowski et al.*, 2008; *Toki et al.*, 2008].

5.2. Processes to Alter δD_{H2} at Low Temperature Environments

[15] A dominant process to control δD values of H₂ in natural thermal fluid is the isotope exchange (equilibrium) reaction [*Proskurowski et al.*, 2006]. Given that the larger isotope fractionation factor at lower temperature (equation (1)) leads to the smaller equilibrated δD_{H2} value at lower temperature assuming $\delta D_{H2O} = +0‰$ (Figure 4), the isotope exchange reaction after the fluid cooling can cause δD_{H2} to shift to a value smaller than that of the HTHFs. This mechanism can explain the δD_{H2} change observed in the LTHF samples. Since the abiotic isotope exchange reaction rate drastically decreases at lower temperatures and the reaction is negligible at 26°C over a month [e.g., *Campbell et al.*, 2009], the significant δD_{H2} change in the LTHFs by the isotope exchange reaction should require some catalysts, such as pure metals. In contrast, subseafloor low temperature environment are favorable for microbial activity, and microbial H₂ metabolisms are known to catalyze the isotope exchanging even at temperatures as low as 30°C [*Romanek et al.*, 2003; *Valentine et al.*, 2004]. Given that H₂ depletion in the LTHFs (Table 1) occurred most likely due to microbial consumption as discussed above, we propose that microbial H₂-consuming activities in the LTHFs are involved in the change of δD_{H2} values (Figure 5). In the CIR Kairei hydrothermal field, the occurrence of active subseafloor hydrogenotrophic methanogenic function by *Methanococcales* and *Methanopyrus* members was demonstrated, particularly along the branching hydrothermal fluid flows [*Takai et al.*, 2004]. The possible subseafloor H₂-oxidizing chemolithoautotrophic activities dominated by *Aquificales* and *Epsilonproteobacteria* members were also suggested in the gas-enriched hydrothermal fluid flows and the ambient environments in the LB Mariner field [*Takai et al.*, 2008a]. The LTHFs obtained from these hydrothermal fields represented lower H₂ concentration and smaller δD_{H2} value compared with those expected at the conservatively mixed fluid (Table 1 and Figures 4 and 5a), suggesting the influence by the isotope exchange activation accompanied with microbial H₂ consumption at subseafloor low-temperature environments. Because all the δD_{H2} values in the LTHFs were still disequilibrated at in situ (measured) temperature and further changeable by the microbial activity if the fluids had longer resided at subseafloor microbial ecosystems, a variety of δD_{H2} values among the LTHF samples (Figure 4) could result from variable fluid residence times and/or microbial activities at low-temperature environment.

[16] The sample ID 932-2 obtained from the CIR Edmond field represented a highly deuterium-depleted δD_{H2} value and an excess amount of H₂ that was fivefold the amount expected from the conservative mixing (Table 1). This
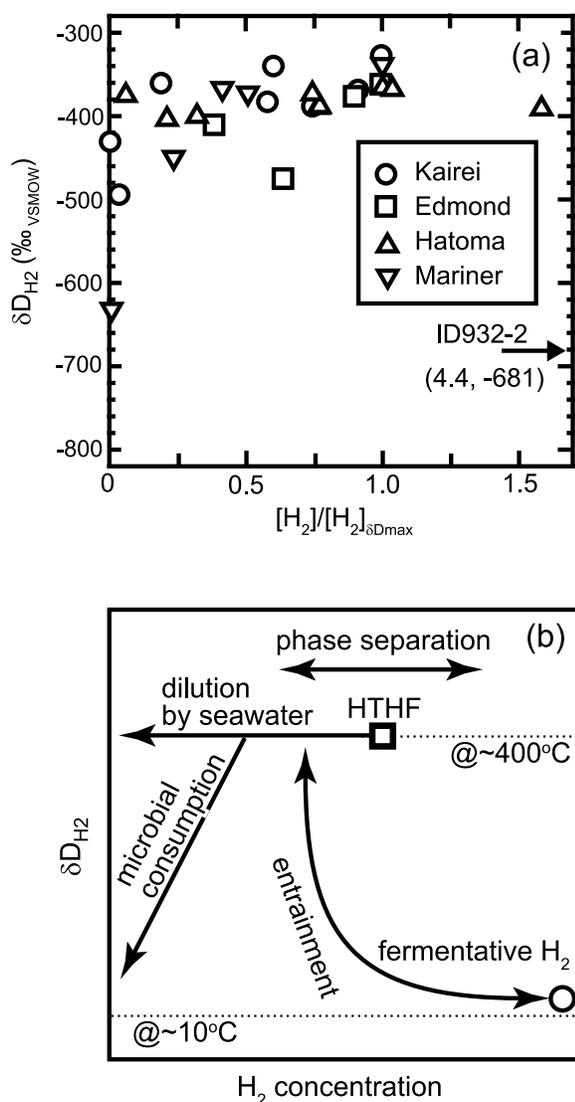
Figure 5. (a) Relationship between H_2 concentration and δD_{H2} values. H_2 concentrations are shown in the standardized values by H_2 concentration of the sample having the maximum δD_{H2} value (considered as the most nearly end-member fluid) for each field. (b) Schematic illustration showing the changes of H_2 concentration and δD_{H2} values against the processes occurring at around hydrothermal systems discussed in this study. A square "HTHF" and a circle "fermentative H_2" represent an end-member high-temperature hydrothermal fluid and H_2 produced by microbial fermentation, respectively. Typical behavior against each process is presented by arrows. Horizontal dotted-lines with temperature indicate the theoretically equilibrated δD_{H2} values at the temperature.

cannot be explained by microbial H_2-consuming activity. The H_2 enrichment with D-depleted δD_{H2} value suggests that the abundant H_2 with a highly deuterium-depleted isotopic signature mixes with hydrothermal fluids around the *Rimicaris* shrimp colony. Microbial fermentative hydrogenogenesis in the *Rimicaris* shrimp colony is one of the possible processes to account for the observed deuterium-

depleted H_2 enrichment. Occurring as a minor process in anaerobic microhabitats, fermentative hydrogenogenesis could occur in any of the natural microbial communities, but as a major process that requires dense microbial populations in anaerobic, organic-matter-rich environments [*Jackson and McInerney*, 2002; *Chou et al.*, 2008]. In deep-sea hydrothermal environments, the chimney surfaces, microbial mats in the solid surfaces and dense animal communities harbor considerable populations of hydrogenogenic fermentative microorganisms [e.g., *Nakagawa and Takai*, 2006]. Molecular hydrogen produced by such microorganisms probably has a δD_{H2} value representing the isotopic equilibrium at the in situ temperature because of involvement of the enzyme hydrogenase [*Vignais*, 2005]. Since the δD value of H_2 produced by fermentative hydrogenogens is estimated at around −750‰ based on equation (1) from the *Rimicaris* shrimps' living temperatures of around 10°–20°C [*van Dover et al.*, 2001], the δD_{H2} value (−681‰) determined in the sample ID932-2 would be simply explained by mixing of H_2 between the HTHF and the fermentative products (Table 1 and Figure 5). This model requires H_2 concentration of the colony water as high as 2 mmol/kg when a mixing between HTHF and the colony water is assumed, although stripping and entrainment of fermentation-derived bubbles absorbed on crust and/or animal bodies by the flowing fluid could result in the observed H_2 enrichment without relation to H_2 concentration in the colony water. In contrast to the biological process, H_2 production through thermal decomposition of organic matter [*Seewald et al.*, 1994] and pyrite formation [*Schoonen et al.*, 1999] potentially occurs at the venting fluid temperature (281°C) and accounts for the H_2 enrichment, but a highly deuterium-depleted isotopic ratio suggests low-temperature H_2 generation and seems unlikely at these high temperature processes. Low-temperature H_2 generation by the reaction of sampled fluid with stainless steel inner wall of the sampler may explain the anomalously high H_2 concentration with the small δD_{H2} value in the sample ID932-2, whereas the observation at OT Hatoma Knoll field denied it as discussed below.

[17] The δD_{H2} values in the Hatoma Knoll field ranged narrow, although anomalously positive H_2 concentration (ID 999-2) and H_2/CO_2 ratio (ID 1001-2) were observed (Table 1 and Figure 3). Similar varieties of H_2 concentration and H_2/CO_2 ratio have been observed in the OT Yonaguni Knoll IV hydrothermal field [*Konno et al.*, 2006], where bubble and liquid CO_2 are vented as well as the Hatoma Knoll field. The varieties of chemical composition in the OT Yonaguni Knoll field were explained by different behaviors between chemical species against phase separation (boiling) and liquid CO_2 formation according to their physical and chemical properties [*von Damm*, 1995]. Similar explanation is applicable to the anomalously high H_2 concentration and H_2/CO_2 ratio in the OT Hatoma Knoll field. Although H_2 concentrations and H_2/CO_2 ratios were varied at OT Hatoma Knoll field (Table 1 and Figure 3) due to phase separation and concomitants of bubbles and liquid CO_2, δD_{H2} values were within the narrow range (Figure 5a). This fact suggests that phase separation and subsequent liquid CO_2 formation little caused δD_{H2} change. Moreover, the δD_{H2} values in the OT Hatoma Knoll fluids, indicating the equilibrium at the temperature higher than 300°C, suggested negligible D-depleted H_2 generation by a low-temperature reaction between a

sampled fluid and the stainless-steel sampler. This fact suggests that the anomalous H$_2$ in the sample ID932-2 that showed H$_2$ concentration higher than those at the OT Hatoma Knoll fluids (Table 1) was derived not from unfortunate H$_2$ generation in the low-temperature sampler, but from natural processes occurring at the hydrothermal environments.

[18] This study proposes qualitative behavior of δD_{H2} values at hydrothermal site (Figure 5b) based on the observation of both HTHFs and LTHFs. Although the fluid-seawater mixing and phase separation exert control over H$_2$ concentration but negligible influence on δD_{H2} value, the microbial H$_2$ metabolism could be the most likely process involved in changing the δD_{H2} value through the isotope exchange reaction by means of the catalytic effect of the enzymes involving H$_2$-consuming and/or H$_2$-generating metabolisms. At present, however, it remains quantitatively uncertain how the microbial H$_2$ metabolisms and abiotic processes affect the δD_{H2} change in LTHFs. In order to use the δD_{H2} value as a new biogeochemical tracer, it will be very important to elucidate the kinetic properties of diverse H$_2$ metabolisms in microbial communities occurring in a variety of deep-sea hydrothermal habitats.

6. Conclusions and Implications

[19] A simple and highly sensitive analytical method to determine H$_2$ concentration and δD_{H2} was devised. The method enables us to determine δD_{H2} values not only in H$_2$-enriched HTHFs, but also H$_2$-depleted LTHFs. We observed a narrow range of δD_{H2} values in HTHFs obtained from several hydrothermal systems, as reported previously, indicating the achievement of the hydrogen isotopic equilibrium between H$_2$ and H$_2$O in the hydrothermal end-member fluids. In contrast, a variety of the δD_{H2} values was detected in LTHF samples. Several LTHFs showed apparently D-depleted δD_{H2} values than those in the HTHFs in spite of a negligible δD_{H2} change due to fluid-seawater mixing, suggesting the possibility of δD_{H2} change in the LTHFs and the surrounding environments. We proposed that microbiological H$_2$ consumption and production would account for the observed δD_{H2} change in the LTHFs, although quantitative understanding of the δD_{H2} change induced by the microbial H$_2$ metabolism remains limited. Studies for investigating the relation between H$_2$ consumption rate and δD_{H2} change rate at microbial hydrogenotrophs are required to prove the discussion in this study.

References

Arnason, B. (1977), The hydrogen-water isotope thermometer applied to geothermal areas in Iceland, *Geothermics*, 5, 75–80.

Butterfield, D. A., et al. (2004), Mixing, reaction, and microbial activity in the sub-seafloor revealed by temporal and spatial variation in diffuse flow vents at axial volcano, in *The Subseafloor Biosphere at Mid-Ocean Ridges, Geophys. Monogr. Ser.*, vol. 144, edited by W. S. D. Wilcock et al., pp. 269–289, AGU, Washington, D. C.

Campbell, B. J., et al. (2009), Hydrogen isotopic fractionation in lipid biosynthesis by H$_2$-consuming Desulfobacterium autotrophicum, *Geochim. Cosmochim. Acta*, doi:10.1016/j.gca.2009.1002.1034.

Charlou, J. L., et al. (2002), Geochemistry of high H$_2$ and CH$_4$ vent fluids issuing from ultramafic rocks at the Rainbow hydrothermal field (36°14′N, MAR), *Chem. Geol.*, 191, 345–359.

Chou, C. J., et al. (2008), Hydrogenesis in hyperthermophilic microorganisms: Implications for biofuels, *Metab. Eng.*, 10(6), 394–404.

Gallant, R. M., and K. L. von Damm (2006), Geochemical controls on hydrothermal fluids from the Kairei and Edmond Vent Fields, 23°–25°S, Central Indian Ridge, *Geochem. Geophys. Geosyst.*, 7, Q06018, doi:10.1029/2005GC001067.

Gamo, T., et al. (2001), Chemical characteristics of newly discovered black smoker fluids and associated hydrothermal plumes at the Rodriguez Triple Junction, Central Indian Ridge, *Earth Planet. Sci. Lett.*, 193(3–4), 371–379.

Horibe, Y., and H. Craig (1995), D/H fractionation in the system methane-hydrogen-water, *Geochim. Cosmochim. Acta*, 59(24), 5209–5217.

Jackson, B. E., and M. J. McInerney (2002), Anaerobic microbial metabolism can proceed close to thermodynamic limits, *Nature*, 415(6870), 454–456.

Kawagucci, S., et al. (2005), An analytical system for determining $\delta^{17}O$ in CO$_2$ using continuous flow-isotope ratio MS, *Anal. Chem.*, 77(14), 4509–4514.

Konno, U., et al. (2006), Liquid CO$_2$ venting on the seafloor: Yonaguni knoll IV hydrothermal system, Okinawa Trough, *Geophys. Res. Lett.*, 33, L16607, doi:10.1029/2006GL026115.

Kumagai, H., et al. (2008), Geological background of the Kairei and Edmond hydrothermal fields along the Central Indian Ridge: Implications of their vent fluids' distinct chemistry, *Geofluids*, 8(4), 239–251.

McCollom, T. M. (1999), Methanogenesis as a potential source of chemical energy for primary biomass production by autotrophic organisms in hydrothermal systems on Europa, *J. Geophys. Res.*, 104(E12), 30,729–30,742.

McCollom, T. M., and J. S. Seewald (2006), Carbon isotope composition of organic compounds produced by abiotic synthesis under hydrothermal conditions, *Earth Planet. Sci. Lett.*, 243, 74–84.

McCollom, T. M., and E. L. Shock (1997), Geochemical constraints on chemolithoautotrophic metabolism by microorganisms in seafloor hydrothermal systems, *Geochim. Cosmochim. Acta*, 61, 4375–4391.

Merlivat, L., F. Pineau, and M. Javoy (1987), Hydrothermal vent waters at 13°N on the East Pacific Rise: Isotopic composition and gas concentration, *Earth Planet. Sci. Lett.*, 84, 100–108.

Moore, R. M., S. Punshon, C. Mahaffey, and D. Karl (2009), The relationship between dissolved hydrogen and nitrogen fixation in ocean waters, *Deep Sea Res., Part I*, 56(9), 1449–1458.

Nakagawa, S., and K. Takai (2006), The isolation of thermophiles from deep-sea hydrothermal environments, in *Extremophiles: Methods in Microbiology*, vol. 35, edited by F. A. Rainey and A. Oren, pp. 57–91, Elsevier, London.

Nakamura, K., et al. (2009), Serpentinized trOctolites exposed near the Kairei Hydrothermal Field, Central Indian Ridge: Insights into the origin of the Kairei hydrothermal fluid supporting a unique microbial ecosystem, *Earth Planet. Sci. Lett.*, 280, 128–136.

Nakano, A., M. Matsumura, and J. Ishibashi (2001), Geochemistry of hydrothermal fluids from the Hatoma Knoll in the South Okinawa Trough (in Japanese with English abstract), *JAMSTEC J. Deep Sea Res.*, 18, 139–144.

Proskurowski, G., et al. (2006), Low temperature volatile production at the Lost City Hydrothermal Field, evidence from a hydrogen stable isotope geothermometer, *Chem. Geol.*, 229(4), 331–343.

Proskurowski, G., et al. (2008), Stable isotopic evidence in support of active microbial methane cycling in low-temperature diffuse flow vents at 9°50′N East Pacific Rise, *Geochim. Cosmochim. Acta*, 72(8), 2005–2023.

Punshon, S., and R. M. Moore (2008a), Photochemical production of molecular hydrogen in lake water and coastal seawater, *Mar. Chem.*, 108, 215–220.

Punshon, S., and R. M. Moore (2008b), Aerobic hydrogen production and dinitrogen fixation in the marine cyanobacterium Trichodesmium erythraeum IMS101, *Limnol. Oceanogr.*, 53, 2749–2753.

Punshon, S., R. M. Moore, and H. X. Xie (2007), Net loss rates and distribution of molecular hydrogen (H$_2$) in mid-latitude coastal waters, *Mar. Chem.*, 105(1–2), 129–139.

Rahn, T., et al. (2002), D/H ratios of atmospheric H$_2$ in urban air: Results using new methods for analysis of nano-molar H$_2$ samples, *Geochim. Cosmochim. Acta*, 66(14), 2475–2481.

Rhee, T. S., et al. (2004), Continuous-flow isotope analysis of the deuterium/hydrogen ratio in atmospheric hydrogen, *Rapid Commun. Mass Spectrom.*, *18*(3), 299–306.

Romanek, C. S., et al. (2003), Carbon and hydrogen isotope fractionations associated with dissimilatory iron-reducing bacteria, *Chem. Geol.*, *195*(1–4), 5–16.

Saegusa, S., et al. (2006), Development of a multibottle gas-tight fluid sampler WHATS II for Japanese submersibles/ROVs, *Geofluids*, *6*(3), 234–240.

Schoonen, M. A. A., Y. Xu, and J. Bebie (1999), Energetics and kinetics of the prebiotic synthesis of simple organic acids and amino acids with the FeS-H₂S/FeS₂ redox couple as reductant, *Origins Life Evol. Biosphere*, *29*(1), 5–32.

Seewald, J. S., W. E. Seyfried, and W. C. Shanks (1994), Variations in the chemical and stable-isotope composition of carbon and sulfur species during organic-rich sediment alteration: An experimental and theoretical study of hydrothermal activity at Guaymas Basin, Gulf of California, *Geochim. Cosmochim. Acta*, *58*(22), 5065–5082.

Shanks, W. C., III, J. K. Bohlke, and R. R. Seal II (1995), Stable isotopes in mid-ocean ridge hydrothermal systems; interactions between fluids, minerals, and organisms, in *Seafloor Hydrothermal Systems: Physical, Chemical, Biological, and Geological Interactions*, *Geophys. Monogr. Ser.*, vol. 91, edited by S. E. Humphris et al., pp. 194–221, AGU, Washington, D. C.

Takai, K., et al. (2004), Geochemical and microbiological evidence for a hydrogen-based, hyperthermophilic subsurface lithoautotrophic microbial ecosystem (HyperSLiME) beneath an active deep-sea hydrothermal field, *Extremophiles*, *8*(4), 269–282.

Takai, K., et al. (2006), Ultramafics-Hydrothermalism-Hydrogenesis-HyperSLiME (UltraH[3]) linkage: A key insight into early microbial ecosystem in the Archean deep-sea hydrothermal systems, *Paleontol. Res.*, *10*, 269–282.

Takai, K., et al. (2008a), Variability in the microbial communities and hydrothermal fluid chemistry at the newly discovered Mariner hydrothermal field, southern Lau Basin, *J. Geophys. Res.*, *113*, G02031, doi:10.1029/2007JG000636.

Takai, K., K. Nakamura, T. Toki, U. Tsunogai, M. Miyazaki, H. Hirayama, S. Nakagawa, T. Nunoura, and K. Horikoshi (2008b), Cell proliferation at 122°C and isotopically heavy CH₄ by a hyperthermophilic methanogen under high pressures cultivation, *Proc. Natl. Acad. Sci. U. S. A.*, *105*, 10,949–10,954.

Toki, T., et al. (2008), Methane enrichment in low-temperature hydrothermal fluids from the Suiyo Seamount in the Izu-Bonin Arc of the western Pacific Ocean, *J. Geophys. Res.*, *113*, B08S13, doi:10.1029/2007JB005476.

Tsunogai, U., F. Nakagawa, T. Gamo, and J. Ishibashi (2005), Stable isotopic compositions of methane and carbon monoxide in the Suiyo hydrothermal plume, Izu-Bonin arc: Tracers for microbial consumption/production, *Earth Planet. Sci. Lett.*, *237*(3–4), 326–340.

Ueno, Y., K. Yamada, N. Yoshida, S. Maruyama, and Y. Isozaki (2006), Evidence from fluid inclusions for microbial methanogenesis in the early Archaean era, *Nature*, *440*, 516–519.

Valentine, D. L., et al. (2004), Hydrogen isotope fractionation during H₂/CO₂ acetogenesis: Hydrogen utilization efficiency and the origin of lipid-bound hydrogen, *Geobiology*, *2*, 179–188.

van Dover, C. L., et al. (2001), Biogeography and ecological setting of Indian Ocean hydrothermal vents, *Science*, *294*(5543), 818–823.

Vignais, P. M. (2005), H/D exchange reactions and mechanistic aspects of the hydrogenases, *Coord. Chem. Rev.*, *249*(15–16), 1677–1690.

von Damm, K. L. (1995), Controls on the chemistry and temporal variability of seafloor hydrothermal fluids, in *Seafloor Hydrothermal Systems: Physical, Chemical, Biological, and Geological Interactions*, *Geophys. Monogr. Ser.*, vol. 91, edited by S. E. Humphris et al., pp. 222–247, AGU, Washington, D. C.

von Damm, K. L., and M. D. Lilley (2004), Diffuse flow hydrothermal fluids from 9°50′N East Pacific Rise: Origin, evolution and biogeochemical controls, in *The Subseafloor Biosphere at Mid-Ocean Ridges*, *Geophys. Monogr. Ser.*, vol. 144, edited by W. S. D. Wilcock et al., pp. 245–268, AGU, Washington, D. C.

Welhan, J. A., and H. Craig (1983), Methane, hydrogen and helium in hydrothermal fluids at 21 degrees N on the East Pacific Rise, in *Hydrothermal Processes at Seafloor Spreading Centers*, edited by P. A. Rona et al., pp. 391–409, Plenum, New York.

T. Gamo, Atmosphere and Ocean Research Institute, University of Tokyo, 5-1-5 Kashiwanoha, Kashiwa, Chiba 277-8564, Japan.

J. Ishibashi, Faculty of Sciences, Kyusyu University, 6-10-1 Hakozaki, Higashi, Fukuoka 812-8581, Japan.

M. Ito, T. Oomori, and T. Toki, Faculty of Science, University of the Ryukyus, 1 Senbaru, Nishihara, Okinawa 903-0213, Japan.

S. Kawagucci, Precambrian Ecosystem Laboratory, Japan Agency for Marine-Earth Science and Technology, 2-15 Natsushima-cho, Yokosuka 237-0061, Japan. (kawagucci@jamstec.go.jp)

K. Takai, Subsurface Geobiology Advanced Research Project, Japan Agency for Marine-Earth Science and Technology, 2-15 Natsushima-cho, Yokosuka 237-0061, Japan.